

Measuring the Leptonic CP Phase in Neutrino Oscillations with Non-Unitary Mixing

Shao-Feng Ge ^{1,*}, Pedro Pasquini ^{2,3,†}, M. Tórtola ^{2,‡} and J. W. F. Valle ^{2§}

¹ *Max-Planck-Institut für Kernphysik, Heidelberg 69117, Germany*

² *AHEP Group, Institut de Física Corpuscular –*

C.S.I.C./Universitat de València, Parc Científic de Paterna.

C/Catedrático José Beltrán, 2 E-46980 Paterna (València) - SPAIN and

³ *Instituto de Física Gleb Wataghin - UNICAMP, 13083-859, Campinas SP, Brazil*

Abstract

Non-unitary neutrino mixing implies an extra CP violating phase that can fake the leptonic Dirac CP phase δ_{CP} of the simplest three-neutrino mixing benchmark scheme. This would hinder the possibility of probing for CP violation in accelerator-type experiments. We take T2K and T2HK as examples to demonstrate the degeneracy between the “standard” (or “unitary”) and “non-unitary” CP phases. We find, under the assumption of non-unitary mixing, that their CP sensitivities severely deteriorate. Fortunately, the TNT2K proposal of supplementing T2(H)K with a μ DAR source for better measurement of δ_{CP} can partially break the CP degeneracy by probing both $\cos \delta_{CP}$ and $\sin \delta_{CP}$ dependences in the wide spectrum of the μ DAR flux. We also show that the further addition of a near detector to the μ DAR setup can eliminate the degeneracy completely.

* gesf02@gmail.com

† pasquini@ifi.unicamp.br

‡ mariam@ific.uv.es

§ valle@ific.uv.es, URL: <http://astroparticles.es/>

I. INTRODUCTION

The search for leptonic CP violation constitutes one of the major challenges in particle physics today [1]. Although CP violation studies are interesting in their own right, they may also shed light upon the general CP symmetries of the neutrino mass matrices in a rather model-independent way [2], such as the case of the generalized $\mu - \tau$ reflection symmetry [3]. Likewise, they can probe the predictions made by specific flavor models and hence put to test the structure of the corresponding symmetries [4, 5].

In analogy with the CP violation present in the CKM mixing matrix describing the quark weak interactions [6–8], massive neutrino schemes lead to leptonic CP violation which affects lepton number conserving processes such as neutrino oscillations. This type of CP violation is associated with the Dirac phase δ_{CP} present in the simplest three-neutrino mixing matrix, which is simply the leptonic analogue of the CKM phase. So far neutrino oscillation experiments have measured the two squared neutrino mass differences, as well as the three corresponding mixing angles [9]. These measurements provide a rather precise determination of all neutrino oscillation parameters, except for the atmospheric mixing angle θ_{23} , whose octant is still uncertain, and the leptonic Dirac CP phase δ_{CP} , which is poorly determined [10]. The precision era in neutrino physics has come with new experimental setups that will provide enough statistics for measuring all of the neutrino parameters to an unprecedented level of accuracy. These include T2K [11], Hyper-K [12], and TNT2K [13]. The TNT2K (Tokai 'N Toyama to Kamioka) project is a combination of μ Kam (with μ DAR source and Super-K (μ SK) or Hyper-K (μ HK) detectors at Kamioka) and T2(H)K. These facilities aim at measuring δ_{CP} .

One is likely to depart from such a simple picture, however, if neutrinos get their mass *a la seesaw*. In this case, neutrino mass arises through the tree level exchange of heavy, so far undetected, $SU(3)_c \otimes SU(2)_L \otimes U(1)_Y$ singlet messenger fermions such as “right-handed” neutrinos, as in the type-I seesaw mechanism. If the seesaw scheme responsible for generating neutrino mass is accessible to the LHC, then it is natural to expect that neutrino oscillations will be described by a non-unitary mixing matrix. Examples of such mechanisms are the inverse and linear seesaw schemes [14–19]. In these schemes one expects sizeable deviations from the simplest three-neutrino benchmark, in which there are only three families of orthonormal neutrinos.

The generic structure of the leptonic weak interaction was first given in Ref. [7] and contains new parameters in addition to those of the simplest three-neutrino paradigm. In this case the description of neutrino oscillations involves an effectively non-unitary mixing matrix [20]. As a consequence, there are degeneracies in the neutrino oscillation probability involving the “standard” three-neutrino CP phase and the “new” phase combination arising

from the non-unitarity of the neutrino mixing matrix [21, 22]. In this paper we examine some strategies to lift the degeneracies present between “standard” and “new” leptonic CP violation effects, so as to extract with precision the Dirac CP phase from neutrino oscillations in the presence of non-unitary mixing. Such effort also provides an indirect way to help probing the mass scale involved in neutrino mass generation through the seesaw mechanism. A precise measurement of the genuine Dirac CP phase would also provide direct tests of residual symmetries that can predict correlation between the Dirac CP phase and the mixing angles [23–27].

Note also that probing the non-unitarity of the neutrino mixing matrix in oscillation searches could provide indirect indications for the associated (relatively low-mass) seesaw messenger responsible for inducing neutrino mass. This would also suggest that the corresponding charged lepton flavour violation and CP violation processes could be sizeable, irrespective of the observed smallness of neutrino masses [28–32]. The spectrum of possibilities becomes even richer in low-scale seesaw theories beyond the $SU(3)_c \otimes SU(2)_L \otimes U(1)_Y$ gauge structure [33, 34]. Unfortunately, however, no firm model-independent predictions can be made in the charged sector. As a result searches for the exotic features such as non-unitary neutrino propagation effects may provide a unique and irreplaceable probe of the theory that lies behind the canonical three-neutrino benchmark.

This paper is organized as follows. In Sec. II we summarize the generalized formalism describing neutrino mixing in the presence of non-unitarity. This convenient parametrization is then used to derive the non-unitarity effects upon the three-neutrino oscillation probabilities, by decomposing their dependence on the CP phases and the atmospheric mixing angle θ_a , see details in App. A. This is useful to demonstrate, in Sec. III, that the size of the non-unitary CP effects can be as large as the standard CP terms, given the current limits on leptonic unitarity violation. In addition, we also implement the inclusion of matter effects [35, 36], as detailed in App. B, and illustrate how they can modify the oscillation probabilities. With the formalism established, we show explicitly in Sec. IV how the “non-unitary” CP phase can fake the standard “unitary” one at accelerator neutrino experiments like T2(H)K. In Sec. V we show that the degeneracy between unitary and non-unitary CP phases can be partially resolved with TNT2K. Moreover, we further propose a near detector μ Near, with 20 ton of liquid scintillator and 20 m of baseline, in order to disentangle the effects of the two physical CP phases and recover the full δ_{CP} sensitivity at TNT2K. Our numerical simulations for T2H(K), μ SK, μ HK, and μ Near are carried out with the NuPro package [37]. The conclusion of this paper can be found in Sec. VI.

II. NEUTRINO MIXING FORMALISM

Within the standard three-neutrino benchmark scheme the neutrino flavor and mass eigenstates are connected by a unitary mixing matrix U [38],

$$\nu_\alpha = U_{\alpha i} \nu_i, \quad (1)$$

where we use the subscript α for flavor and i for mass eigenstates. This lepton mixing matrix may be expressed as

$$U = \mathcal{P} \begin{pmatrix} c_s c_r & s_s c_r & s_r e^{-i\delta_{CP}} \\ -c_a s_s - s_a s_r c_s e^{i\delta_{CP}} & c_a c_s - s_a s_r s_s e^{i\delta_{CP}} & s_a c_r \\ s_a s_s - c_a s_r c_s e^{i\delta_{CP}} & -s_a c_s - c_a s_r s_s e^{i\delta_{CP}} & c_a c_r \end{pmatrix} \mathcal{Q}. \quad (2)$$

in which we have adopted the PDG variant [39] of the original symmetric parametrization of the neutrino mixing matrix [7], with the three mixing angles θ_{12} , θ_{23} and θ_{13} denoted as θ_s , θ_a and θ_r , for solar, atmospheric and reactor, respectively. Within this description, three of the CP phases in the diagonal matrices $\mathcal{P} \equiv \text{diag}\{e^{-i\beta_1}, e^{-i\beta_2}, e^{-i\beta_3}\}$ and $\mathcal{Q} \equiv \text{diag}\{e^{-i\alpha_1}, e^{-i\alpha_2}, e^{-i\alpha_3}\}$ can be eliminated by redefining the charged lepton fields, while one is an overall phase that can be rotated away. The remaining phases correspond to the two physical Majorana phases [7]¹. This leaves only the Dirac CP-phase δ_{CP} characterizing CP violation in neutrino oscillations.

If neutrinos acquire mass from the general seesaw mechanism through the exchange of $SU(3)_c \otimes SU(2)_L \otimes U(1)_Y$ singlet heavy messenger fermions, these extra neutrino states mix with the standard ν_e , ν_μ , ν_τ , and then the neutrino mixing needs to be extended to go beyond 3×3 ,

$$U^{n \times n} = \begin{pmatrix} N & W \\ V & T \end{pmatrix}, \quad (3)$$

Note that the total mixing matrix $U^{n \times n}$ (with $n > 3$) shall always be unitary, regardless of its size. The leptonic weak interaction mixing matrix is promoted to rectangular form [7] where each block can be systematically determined within the seesaw expansion [43]. However if the extra neutrinos are heavy they cannot be produced at low energy experiments nor will be accessible to oscillations. In such case only the first 3×3 block N can be visible [44–46]. In other words, the original 3×3 unitary mixing U in (2) is replaced by a truncated non-unitary mixing matrix N which will effectively describe neutrino propagation. This can be

¹ The absence of invariance under rephasings of the Majorana neutrino Lagrangean leaves these extra two physical Majorana phases [7]. They do not affect oscillations [40, 41], entering only in lepton number violation processes, such as neutrinoless double beta decay or $0\nu\beta\beta$ [42].

written as

$$N = N^{NP}U = \begin{pmatrix} \alpha_{11} & 0 & 0 \\ \alpha_{21} & \alpha_{22} & 0 \\ \alpha_{31} & \alpha_{32} & \alpha_{33} \end{pmatrix} U. \quad (4)$$

This convenient parametrization follows from the symmetric one in [7] and applies for any number of additional neutrino states [20]. Irrespective of the number of heavy singlet neutrinos, it involves three real parameters (α_{11}, α_{22} and α_{33} , all close to one) and three small complex parameters (α_{21}, α_{31} and α_{32}). In the standard model one has, of course, $\alpha_{ii} = 1$ and $\alpha_{ij} = 0$ for $i \neq j$. Current experiments, mainly involving electron and muon neutrinos, are sensitive to three of these parameters: α_{11}, α_{22} and α_{21} . Note that the latter is complex and therefore we end up with three additional real parameters and one new complex phase

$$\phi \equiv -\arg(\alpha_{21}).$$

The above definition matches the notation in Refs. [20, 21]. Updated constraints on those unitarity violation parameters at 90% C.L. were given in [20],

$$\alpha_{11}^2 \geq 0.989, \quad \alpha_{22}^2 \geq 0.999, \quad |\alpha_{21}|^2 \leq 6.6 \times 10^{-4}, \quad (5)$$

No sensitivity on the non-unitary CP phase ϕ has been obtained so far. Each individual bound has been obtained after marginalizing over the remaining parameters. To accommodate the full correlation between the non-unitarity parameters in our calculations one needs to consider the original constraints [20],

$$\left(\frac{G_\beta}{G_\mu}\right)^2 = \frac{1}{\alpha_{22}^2 + |\alpha_{21}|^2} = 0.9999 \pm 0.0006 \quad @ 1\sigma, \quad (6a)$$

$$\frac{R_\pi}{R_\pi^{SM}} = \frac{\alpha_{11}^2}{\alpha_{22}^2 + |\alpha_{21}|^2} = 0.9956 \pm 0.0040 \quad @ 1\sigma, \quad (6b)$$

$$[\sin^2(2\theta_{\mu e})]_{eff} = 2\alpha_{11}^2 |\alpha_{21}|^2 \leq 0.0014 \quad @ 90\% \text{C.L.} \quad (6c)$$

Therefore, we have implemented these bounds as priors in the NuPro package [37].

III. EFFECT OF THE NON-UNITARITY CP PHASE

As demonstrated in [47], the three currently unknown parameters in neutrino oscillations, the neutrino mass hierarchy, the leptonic Dirac CP phase δ_{CP} , and the octant of the atmospheric angle θ_a , can be analytically disentangled from each other. This decomposition formalism is extremely useful to study the effect of different unknown parameters in various types of neutrino oscillation experiments. Here, we generalize the formalism to accommodate the effect of non-unitary neutrino mixing, $N = N^{NP}U$, as parametrized in Eq. (4). This

extra mixing can be factorized from the Hamiltonian \mathcal{H}^{NP} and the oscillation amplitude S^{NP} , together with $U_{23}(\theta_a)$, which is the 2–3 mixing due to the atmospheric angle θ_a , and the rephasing matrix $P_\delta \equiv \text{diag}(1, 1, e^{i\delta_{CP}})$,

$$\mathcal{H}^{NP} = [N^{NP}U_{23}(\theta_a)P_\delta]\mathcal{H}'[N^{NP}U_{23}(\theta_a)P_\delta]^\dagger, \quad (7a)$$

$$S^{NP} = [N^{NP}U_{23}(\theta_a)P_\delta]S'[N^{NP}U_{23}(\theta_a)P_\delta]^\dagger. \quad (7b)$$

With less mixing parameters, it is much easier to first evaluate S' with the transformed Hamiltonian \mathcal{H}' . The effect of the non-unitary mixing parameters in N^{NP} , the atmospheric angle θ_a and the Dirac CP phase δ_{CP} can then be retrieved in an analytical way (see App. A for more details).

Here, we find that the key oscillation probability $P_{\mu e}$ for the $\nu_\mu \rightarrow \nu_e$ channel is given by,

$$P_{\mu e}^{NP} = \alpha_{11}^2 \{ \alpha_{22}^2 [c_a^2 |S'_{12}|^2 + s_a^2 |S'_{13}|^2 + 2c_a s_a (\cos \delta_{CP} \mathbb{R} - \sin \delta_{CP} \mathbb{I})(S'_{12} S'_{13}^*)] + |\alpha_{21}|^2 P_{ee} \\ + 2\alpha_{22} |\alpha_{21}| [c_a (c_\phi \mathbb{R} - s_\phi \mathbb{I})(S'_{11} S'_{12}^*) + s_a (c_{\phi+\delta_{CP}} \mathbb{R} - s_{\phi+\delta_{CP}} \mathbb{I})(S'_{11} S'_{13}^*)] \}. \quad (8)$$

The choice of this parametrization is extremely convenient to separate the neutrino oscillation probabilities into several terms, as we further elaborate in App. A. In this formalism, the transition probability $P_{\mu e}^{NP}$ relevant for the CP studies can be decomposed into several terms, $P_{\mu e}^{NP} = \sum_k f_k(\alpha_{ij}, \theta_a, \phi) P_{\mu e}^{(k)}(S')$. It contains six terms $P_{\mu e}^{(2,3,7,8,9,10)}$ involving the Dirac CP phases δ_{CP} and ϕ (see Table I in App. A). The standard phase δ_{CP} is modulated by $P_{\mu e}^{(2,3)}$, which are mainly controlled by the matrix elements $(\mathbb{R}, \mathbb{I})(S'_{12} S'_{13}^*)$, while the non-unitarity counterparts $P_{\mu e}^{(7,8,9,10)}$ involve the elements $(\mathbb{R}, \mathbb{I})(S'_{11} S'_{12}^*, S'_{11} S'_{13}^*)$.

If $(\mathbb{R}, \mathbb{I})(S'_{11} S'_{12}^*, S'_{11} S'_{13}^*)$ are of the same size as $(\mathbb{R}, \mathbb{I})(S'_{12} S'_{13}^*)$, the effect of the non-unitary CP phase ϕ is then suppressed by the constraint $|\alpha_{21}| \lesssim 0.026$. Nevertheless, S'_{11} has much larger magnitude than S'_{12} and S'_{13} which becomes evident by calculating the amplitude matrix S' in the basis in which the atmospheric angle θ_a and the Dirac CP phase are factorized. Since the matter effects are small for the experiments under consideration, here we can illustrate the picture with the result in vacuum ²,

$$S' = \mathbb{I}_{3 \times 3} - 2i \sin \Phi_a e^{-i\Phi_a} \begin{pmatrix} s_r^2 & c_r s_r \\ & 0 \\ c_r s_r & c_r^2 \end{pmatrix} - 2i \sin \Phi_s e^{-i\Phi_s} \begin{pmatrix} c_r^2 s_s^2 & c_r c_s s_s & -c_r s_r s_s^2 \\ c_r c_s s_s & c_s^2 & -s_r c_s s_s \\ -c_r s_r s_s^2 & -s_r c_s s_s & s_r^2 s_s^2 \end{pmatrix}, \quad (9)$$

where $\mathbb{I}_{3 \times 3}$ is the 3×3 identity matrix and $\Phi_{a,s} \equiv \Delta m_{a,s}^2 / 4E_\nu$ denote the solar and atmospheric oscillation phases. One can see explicitly that the amplitude matrix S' is symmetric in the absence of matter potential as well as for symmetric matter profiles. For CP measure-

² Although our results are obtained under the assumption that there is no matter effect, they also apply when the matter effect is not significant. See App. B for details.

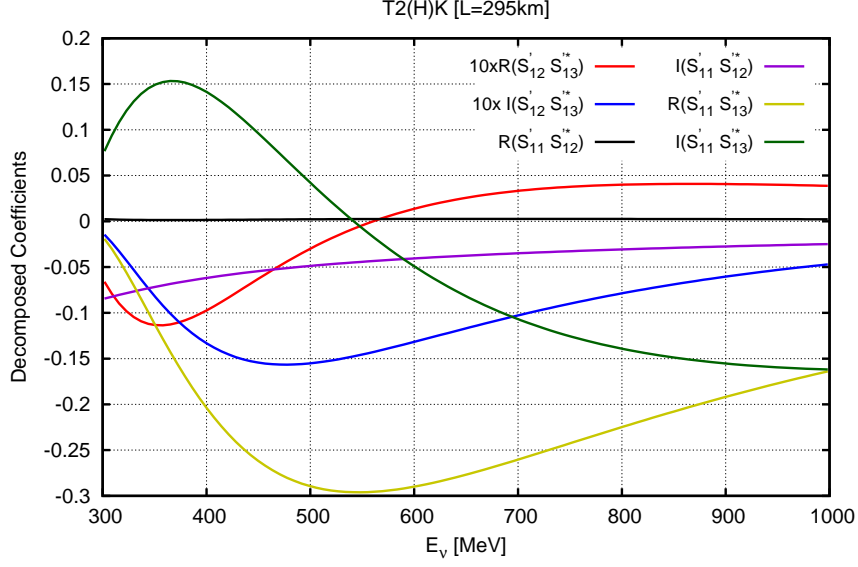


FIG. 1. The decomposed CP coefficients for the neutrino oscillation probability $P_{\mu e}$ for T2(H)K.

ments at accelerator experiments, the neutrino energy and baseline are usually configured around the first oscillation peak, $\Phi_a \approx \frac{\pi}{2}$. Correspondingly, $\Phi_s \approx \frac{\pi}{2} \times \Delta m_s^2 / \Delta m_a^2$, has a small value. Up to leading order, $S'_{11} \approx 1$, in comparison with $S'_{12} \approx -2i \sin \Phi_s e^{-i\Phi_s} c_r c_s s_s$ and $S'_{13} \approx -2i \sin \Phi_a e^{-i\Phi_a} c_r s_r$. The S'_{12} element is suppressed by $\Delta m_s^2 / \Delta m_a^2$ while S'_{13} is suppressed by the reactor angle θ_r . Consequently, the non-unitary elements $\mathbb{I}(S'_{11} S'_{12}^*)$ and $(\mathbb{R}, \mathbb{I})(S'_{11} S'_{13}^*)$ are expected to be at least one order of magnitude larger than the unitary elements $(\mathbb{R}, \mathbb{I})(S'_{12} S'_{13}^*)$. Note that S'_{12} is mainly imaginary, which makes $\mathbb{R}(S'_{11} S'_{12}^*)$ to almost vanish. Among the remaining non-unitary terms, there is still a hierarchical structure. Since S'_{12} is suppressed by $\Delta m_s^2 / \Delta m_a^2$ while S'_{13} is suppressed by s_r , the relative size is roughly $|S'_{12} / S'_{13}| \sim 1/5$. In short, there are five independent CP terms in $P_{\mu e}$, in full agreement with the result in [20]. To give an intuitive picture, we plot in Fig. 1 the six CP related decomposition coefficients at T2(H)K [13] for illustration. The relative size of the coefficients can then be measured by,

$$R_a \equiv \frac{2|\alpha_{21}|}{\alpha_{22}} \frac{\mathbb{R}(S'_{11} S'_{1a}^*) + \mathbb{I}(S'_{11} S'_{1a}^*)}{\mathbb{R}(S'_{12} S'_{13}^*) + \mathbb{I}(S'_{12} S'_{13}^*)}, \quad (10)$$

where $a = 2, 3$. We plot the ratio R_a for $2|\alpha_{21}|/\alpha_{22}^2 = 5\%$ on Fig. 2, where it is even clearer that $\mathbb{I}(S'_{11} S'_{12}^*)$ and $(\mathbb{R}, \mathbb{I})(S'_{11} S'_{13}^*)$ are typically ~ 10 - 20 times larger than $(\mathbb{R}, \mathbb{I})(S'_{12} S'_{13}^*)$, as expected. These considerations show that the size of the standard and the non-unitary contribution can be of the same order. As a result, it can easily mimic the shape of the oscillation curve visible to the experimental setup.

Another intuitive way to observe this is through the plot of oscillation probability as a function of L/E as in Fig. 3. Notice how a non-zero value of ϕ can mimic the behaviour

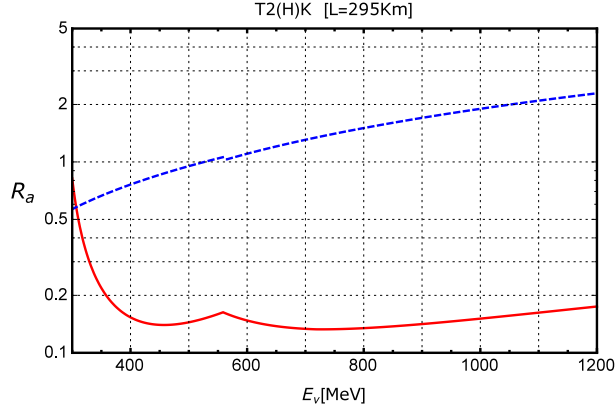


FIG. 2. R_a ratio as given in Eq. (10) for the T2(H)K experimental setup, setting $2|\alpha_{21}|/\alpha_{22} = 5\%$. The solid red line corresponds to R_2 , while R_3 is given by the dashed blue line.

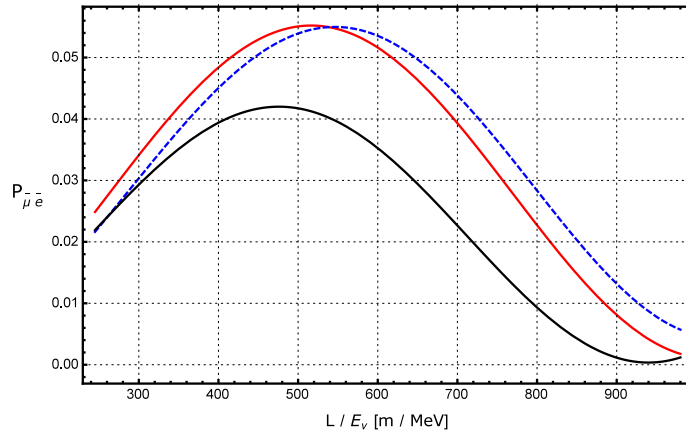


FIG. 3. Electron antineutrino appearance probability as a function of L/E for three different assumptions: (i) black solid line: unitary case with $\delta_{CP} = 0$, (ii) blue dashed line: unitary with $\delta_{CP} = 3\pi/2$, (iii) red solid line: non-unitary case with $\delta_{CP} = 0$, $|\alpha_{21}| = 0.02$ and $\phi = 0.1\pi$.

of $\delta_{CP} = 3\pi/2$ (dashed blue line) even with $\delta_{CP} = 0$ (solid red line). Later on, it will become clear that if the magnitude of the non-unitarity CP effect $|\alpha_{21}|$ is as large as 5%, the standard CP phase δ_{CP} will not be distinguishable from its non-unitary counterpart ϕ , unless the experiment can measure neutrino oscillations over a wide range of L/E . This issue will be taken up and elaborated in Sec. IV.

It should be pointed out that although in the T2K experiment the matter effect is small, it is not completely negligible when considering the sensitivity on the CP phases. The effect of the non-unitary mixing and the matter potential in the electron neutrino appearance probability is shown in Fig. 4. This means that a CP analysis should take matter effects into account: in App. B we present a formalism to deal with matter effects in the context

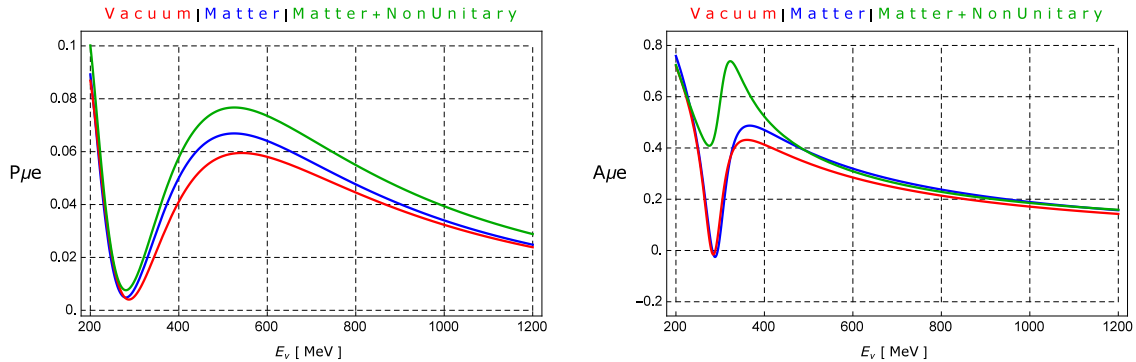


FIG. 4. Left: muon to electron neutrino appearance probability at a baseline of 295 km. Right: the corresponding CP asymmetry between neutrino and anti-neutrino oscillations. We compare three assumptions: unitary mixing in vacuum (red), unitary mixing in matter (blue) and non-unitary mixing in matter with $|\alpha_{21}| = 0.02$ and $\phi = 3\pi/2$ (green). In all cases we take $\delta_{CP} = 3\pi/2$.

of non-unitary neutrino mixing. As a good approximation, one can assume an Earth profile with constant density $\rho_{\text{earth}} = 3 \text{ g/cm}^3$ throughout this paper.

IV. FAKING THE DIRAC CP PHASE WITH NON-UNITARITY

As depicted in Figs. 1 and 2, the size of the amplitude matrix elements $\mathbb{I}(S'_{11}S'_{12}{}^*)$ and $(\mathbb{R}, \mathbb{I})(S'_{11}S'_{13}{}^*)$ that contribute to the CP terms associated to unitarity violation are typically ~ 10 - 20 times larger than their unitary counterparts $(\mathbb{R}, \mathbb{I})(S'_{12}S'_{13}{}^*)$. According to the prior constraints in Eq.(6), the magnitude of the non-unitary CP term $|\alpha_{21}|$ is about 2.6% at 90% C.L. Consequently, after taking into account the extra factor of 2 associated with $|\alpha_{21}|$ in Tab. I, one finds that the non-unitary CP coefficients $P_{\mu e}^{(8,9,10)}$ can be as large as the unitary ones $P_{\mu e}^{(2,3)}$. Hence there is no difficulty for the non-unitary CP phase ϕ to fake the effects normally ascribed to the conventional CP phase δ_{CP} , given the currently available prior constraints on non-unitarity.

In order to study to what extent the standard CP phase δ_{CP} can be faked by the non-unitary CP phase ϕ , we simulate, for illustration, the T2(H)K experiment, as shown in Fig. 5. The pseudo-data are simulated with the true value of $\delta_{CP} = 3\pi/2$, under the assumption of unitary mixing,

$$\delta_{CP}^{true} = 3\pi/2, \quad \alpha_{11}^{true} = \alpha_{22}^{true} = 1, \quad |\alpha_{21}|^{true} = 0. \quad (11)$$

In other words, there is no unitarity violation in the simulated pseudo-data. We assume that T2K can run for 12 years and T2HK for 6 years [13]. This is based on the hypothesis that the HK detector will be built 6 years later than T2K started running, and then T2K

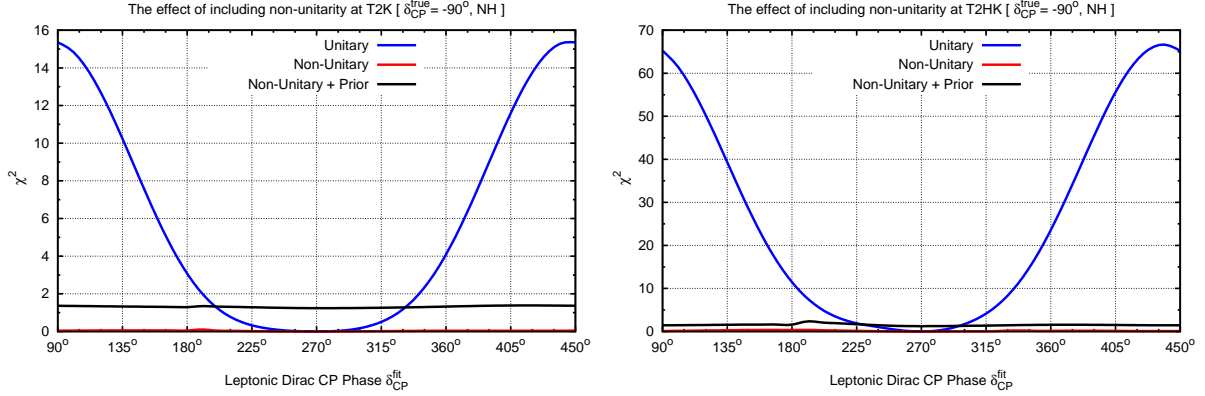


FIG. 5. The marginalized $\chi^2(\delta_{CP})$ function at T2K and T2HK under the assumptions of unitary mixing (blue) and non-unitary mixing with (red) or without (black) prior constraints.

and T2HK can work simultaneously for another 6 years. For both T2K and T2HK, 1/3 of the time is assigned to the neutrino mode and 2/3 to the anti-neutrino channel.

To extract the sensitivity on the leptonic Dirac CP phase δ_{CP} , we fit the pseudo-data with the following χ^2 function,

$$\chi^2 \equiv \chi_{stat}^2 + \chi_{sys}^2 + \chi_{prior}^2, \quad (12)$$

where the three terms (χ_{stat}^2 , χ_{sys}^2 , χ_{prior}^2) stand for the statistical, systematical, and prior contributions. The statistical contribution χ_{stat}^2 comes from the experimental data points,

$$\chi_{stat}^2 = \sum_i \left(\frac{N_i^{\text{pred}} - N_i^{\text{data}}}{\sqrt{N_i^{\text{data}}}} \right)^2, \quad (13)$$

with summation over energy bins, for a specific experiment. For the combined analysis of several experiments, the total χ_{stat}^2 will be a summation over their contributions. In the systematical term χ_{sys}^2 we take into account the flux uncertainties. For T2(H)K, we assume a 5% flux uncertainty for the neutrino and anti-neutrino modes independently,

$$\chi_{sys}^2 = \left(\frac{f_\nu - 1}{0.05} \right)^2 + \left(\frac{f_{\bar{\nu}} - 1}{0.05} \right)^2. \quad (14)$$

Note that both the statistical χ_{stat}^2 and systematical χ_{sys}^2 parts need to be extended when adding extra experiments. In contrast, the prior knowledge is common for different experimental setups. For the discussion that follows, it consists of two parts,

$$\chi_{prior}^2 = \chi_{unitary}^2 + \chi_{non-unitary}^2. \quad (15)$$

The first term $\chi_{unitary}^2$ contains the current measurement of the three-neutrino oscillation parameters [10], as summarized in the Sec.2.1 of [13], while the contribution $\chi_{non-unitary}^2$

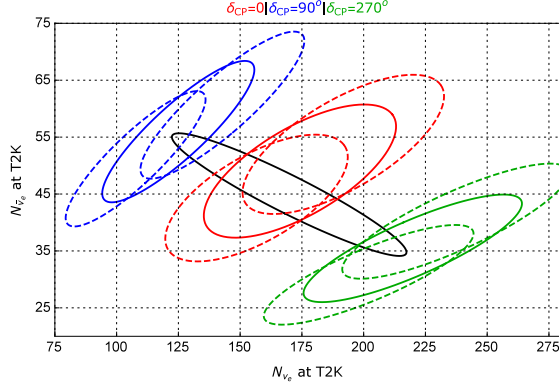


FIG. 6. Bi-event rate plot for T2K for standard three-neutrino mixing with varying δ_{CP} (black line), and non-unitary mixing with fixed δ_{CP} value and varying ϕ (color lines). Dashed lines correspond to $\sin^2 \theta_a = 0.5$ while solid lines correspond to $\sin^2 \theta_a = 0.5 \pm 0.055$.

accounts for the current constraint on the unitarity violating parameters in Eq. (6). Note that the unitary prior contribution $\chi^2_{unitary}$ is always imposed while $\chi^2_{non-unitary}$ is only considered when fitting the data under the non-unitarity assumption with prior constraint.

We then fit the data under different assumptions. For each value of the CP phase δ_{CP} , the marginalized value of χ^2 in Fig. 5 is obtained by first fixing the fit value of δ_{CP} and then minimizing the χ^2 function over the other oscillation parameters. Depending on the assumption, the parameter list includes the three mixing angles, the two mass squared differences, and the non-unitary parameters. The blue curves in Fig. 5 are obtained by assuming standard unitary mixing, with minimization over the three mixing angles ($\theta_a, \theta_r, \theta_s$) and the two mass splittings ($\Delta m_a^2, \Delta m_s^2$). The result is the marginalized $\chi^2(\delta_{CP})$ function from which we can read off the CP measurement sensitivity, $\chi^2(\delta_{CP}) = 1$ for 1σ . One can see that T2K can distinguish reasonably well a nonzero Dirac CP phase from zero, while T2HK can further enhance this sensitivity, under the unitarity assumption. We then turn on the non-unitarity parameters and $\chi^2_{non-unitary}$. As we can see, the situation totally changes once non-unitarity is introduced. The inclusion of the non-unitarity degrees of freedom ($\alpha_{11}, \alpha_{22}, |\alpha_{21}|$, and ϕ) requires the marginalization over nine parameters. Given a nonzero fitting value δ_{CP}^{fit} , one can find a counter-term from the non-unitarity terms $P_{\mu e}^{(8,9,10)}$ that cancel the CP effect arising from the standard terms $P_{\mu e}^{(2,3)}$, leading to better agreement with the pseudo-data. In other words, the effect of the CP phase δ_{CP} can be faked by its non-unitary counterpart ϕ . The resulting $\chi^2(\delta_{CP})$ becomes nearly flat, as shown by the red curves in Fig. 5. Under the assumption of non-unitary mixing, there is almost no CP sensitivity in either T2K or T2HK.

Imposing the correlated prior constraints (6) as $\chi^2_{non-unitary}$ does not improve the situation, as seen in the black curves in Fig. 5. The prior constraints only add a nearly constant

contribution to the $\chi^2(\delta_{CP})$ function, since the best values of non-unitarity parameters according to Eq.(6) differ from the input values for the pseudo-data in Eq. (11). Hence the shape of the $\chi^2(\delta_{CP})$ curve is not affected by the prior constraints. With or without the current prior constraints, neither of the T2K or T2HK experiments by themselves can measure the Dirac CP phase δ_{CP} unambiguously. An intuitive plot to illustrate this fact is presented in Fig. 6 where we show the event rates for the neutrino and antineutrino appearance channel in T2K for two different assumptions: the standard three-neutrino case with varying δ_{CP} (black line), and the alternative non-unitary case with fixed δ_{CP} and varying ϕ (color lines). The variation of the atmospheric angle θ_a has been also considered in the non-unitary case. In particular, dashed lines in the plot correspond to maximal mixing, $\sin^2 \theta_a = 0.5$, while solid lines cover approximately the 1σ allowed range, $\sin^2 \theta_a = 0.5 \pm 0.055$. A similar plot was presented in [21] for $L/E = 500$, in order to understand the origin of the ambiguity in parameter space which is inherent to the problem. Now we show that, for the same baseline $L/E \approx 500$ m/MeV, the uncertainties in the atmospheric mixing angle spoil the good sensitivity to δ_{CP} found after the combination of neutrino and antineutrino channel in Ref. [21]. Moreover, one should keep in mind that, in a realistic case, the existence of flux uncertainties would change each of the ellipses of Fig. 6 into bands.

The reason that the leptonic Dirac CP phase δ_{CP} can be faked by non-unitarity at T2(H)K is due to the choice of narrow neutrino energy spectrum with peak around 550 MeV and baseline at 295 km. With this choice, the oscillation phase $\Phi_a \approx \pi/2$ is almost maximal and the $\cos \delta_{CP}$ term vanishes with its coefficient $\cos \Phi_a$. It is still easy for the CP phase ϕ associated to non-unitarity to fake the standard Dirac phase δ_{CP} , even at the special point pointed in [21], where the degeneracies cancel out in the ideal case of precisely known θ_a and monochromatic energy spectrum. The faking of the standard Dirac CP phase comes from the interplay of various elements. Around the maximal oscillation phase, $\Phi_a \approx \pi/2$, the oscillation probability for neutrinos and anti-neutrinos can be approximated by,

$$P_{\mu e} \approx 4s_a^2 c_r^2 s_r^2 \sin^2 \Phi_a + 2|\alpha_{21}| \Re(S'_{11} S'_{13}{}^*) \cos(\phi + \delta_{CP}) - \Im(S'_{12} S'_{13}{}^*) \sin \delta_{CP} + 2|\alpha_{21}| [\Im(S'_{11} S'_{12}{}^*) \sin \phi - \Im(S'_{11} S'_{13}{}^*) \sin(\phi + \delta_{CP})] , \quad (16a)$$

$$P_{\mu \bar{e}} \approx 4s_a^2 c_r^2 s_r^2 \sin^2 \Phi_a + 2|\alpha_{21}| \Re(S'_{11} S'_{13}{}^*) \cos(\phi + \delta_{CP}) + \Im(S'_{12} S'_{13}{}^*) \sin \delta_{CP} - 2|\alpha_{21}| [\Im(S'_{11} S'_{12}{}^*) \sin \phi - \Im(S'_{11} S'_{13}{}^*) \sin(\phi + \delta_{CP})] , \quad (16b)$$

where the first line is the same both for neutrino and anti-neutrino modes, while the second receives a minus sign. To fit the current experimental best value $\delta_{CP}^{true} = -\pi/2$ with the opposite $\delta_{CP}^{fit} = \pi/2$, the major difference is introduced by the sin terms in the second line. The CP sensitivity is spoiled by freeing θ_a and $|\alpha_{21}|$ and it can be faked by varying ϕ . This introduces a common correction via the $\cos(\phi + \delta_{CP})$ term for both neutrino and

anti-neutrino channels. The large uncertainty in the atmospheric angle, which can reach 10% in s_a^2 , helps to absorb this common correction. The remaining $\sin \phi$ and $\sin(\phi + \delta_{CP})$ terms can then fake the genuine CP term $\sin \delta_{CP}$. Although the coefficients of $\sin \phi$ and $\sin(\phi + \delta_{CP})$ are relatively small, they are not zero. As long as α_{21} is large enough, CP can be faked. This can explain the behavior seen in Fig. 5 and Fig. 6.

V. PROBING CP VIOLATION WITH μ DAR AND NEAR DETECTOR

In order to fully resolve the degeneracy between the unitary and non-unitary CP phases, it is necessary to bring back the $\cos \delta_{CP}$ dependence by carefully choosing the energy spectrum and baseline configuration. A perfect candidate for achieving this is to use muon decay at rest (μ DAR) which has a wide peak and shorter baseline around 15-23 km. The TNT2K experiment [13] is proposed to supplement the existing Super-K detector and the future Hyper-K detector with a μ DAR source. Since the accelerator neutrinos in T2(H)K have higher energy than those of the μ DAR source, the two measurements can run simultaneously. With T2(H)K running solely in the neutrino mode while μ SK and μ HK running in the anti-neutrino mode, the sensitivity to the leptonic Dirac CP phase δ_{CP} can improve significantly. Following [13], we assign 12 years of running for T2K and 6 years for T2HK to run solely in the neutrino mode while μ SK and μ HK have 6 years to run in the anti-neutrino mode. Notice that this experiment has backgrounds from atmospheric neutrinos, from the elastic scattering with electrons, and the quasi-elastic scattering with heavy nuclei. In addition, the μ DAR flux can have 20% uncertainty if there is no near detector. For simplicity, we adopt the same configuration as in [13].

Note also that the sensitivity to break the degeneracy between δ_{CP} and $\pi - \delta_{CP}$ at T2(H)K, arising from the single $\sin \delta_{CP}$ dependence, can be improved because of the wide spectrum of μ DAR, which has both $\cos \delta_{CP}$ and $\sin \delta_{CP}$ dependences as shown in Fig. 7. For the μ DAR flux, the spectrum peaks around 40-50 MeV. In this energy range, the decomposed coefficients $P_{\mu e, e \mu}^{(2)}$ for the $\cos \delta_{CP}$ dependence have comparable magnitude with the $\sin \delta_{CP}$ term coefficients $P_{\mu e, e \mu}^{(3)}$. In contrast, for T2(H)K the coefficients $P_{\mu e, e \mu}^{(2)}$ vanish around the spectrum peak ~ 550 GeV while $P_{\mu e, e \mu}^{(3)}$ have sizable magnitude, as shown in Fig. 1.

The property of having both $\cos \delta_{CP}$ and $\sin \delta_{CP}$ dependences is exactly what we need also to break the degeneracy between the unitary and non-unitary CP phases. As shown in Fig. 8, supplementing T2K with μ SK can preserve the CP sensitivity at the T2K level even if not imposing the prior constraint (6). With prior constraints, the CP sensitivity can further improve beyond that of T2K alone for unitary mixing. The same holds for the T2HK configuration. Nevertheless, the advantage of μ DAR is still not fully utilized.

An important difference between T2(H)K in Fig. 5 and TNT2K in Fig. 8 is the effect

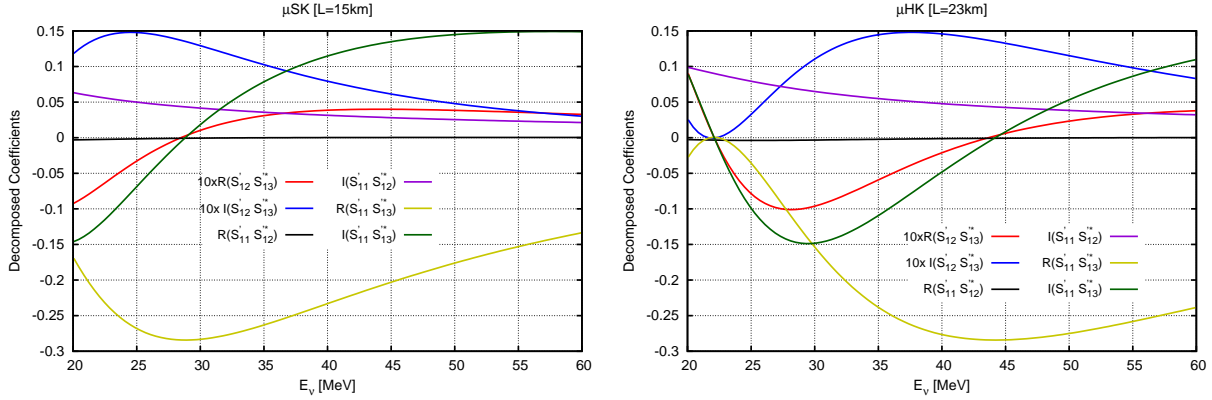


FIG. 7. The amplitude matrix elements S'_{ij} that contribute to the decomposed CP coefficients for the probabilities of anti-neutrino oscillation at μ SK and μ HK.

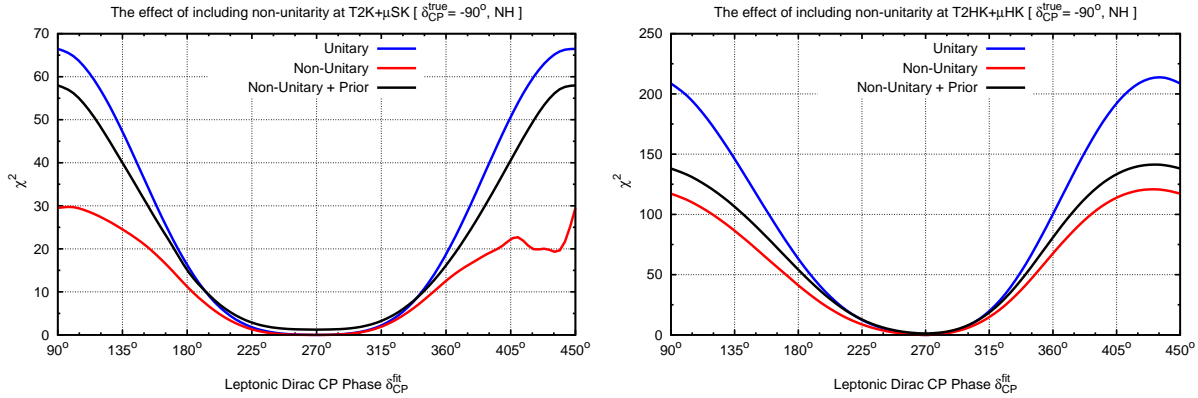


FIG. 8. The marginalized $\chi^2(\delta_{CP})$ function at TNT2K under the assumptions of unitarity (blue), non-unitary mixing with (red) or without (black) prior constraints.

of adding prior constraints. At T2(H)K, prior constraints can only add a nearly flat term to the $\chi^2(\delta_{CP})$ function without improving the CP determination sensitivity. On the other hand, its effect can be maximized at TNT2K after including μ Kam. We find that the CP sensitivity is significantly improved by the combination of μ Kam and prior constraints. Notice in Fig. 9 that the ambiguity of the ellipses was not improved by having another experiment, nevertheless one can distinguish the standard case from the non-unitary case by taking a closer look at the neutrino spectrum which contains more information. Indeed, the advantage of μ Kam is not fully explored with the current prior constraints in (6). Since the non-unitary CP effect is modulated by $|\alpha_{21}|$, a more stringent constraint on $|\alpha_{21}|$ would effectively suppress the size of the faked CP violation. From the expression of $P_{\mu e}^{NP}$ in Eq. (A5c), one sees that if the oscillation baseline is extremely short, it is dominated by the last term

$$P_{\mu e}^{NP} \approx \alpha_{11}^2 |\alpha_{21}|^2, \quad (17)$$

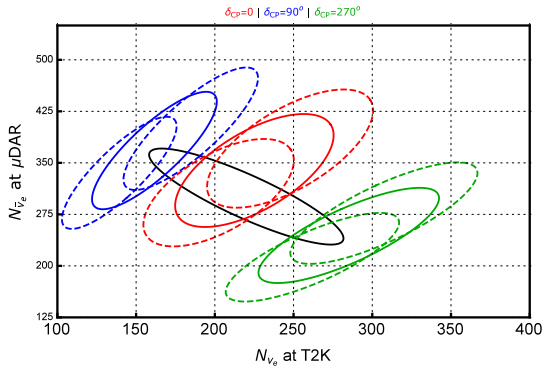


FIG. 9. Bi-event rate plot for TNT2K for standard three-neutrino mixing with varying δ_{CP} (black line), and non-unitary mixing with fixed δ_{CP} value and varying ϕ (color lines). Dashed lines correspond to $\sin^2 \theta_a = 0.5$ while solid lines correspond to $\sin^2 \theta_a = 0.5 \pm 0.055$.

which is a nonzero constant. Such “zero-distance effect” is a direct measure of the effective non-orthonormality of weak-basis neutrinos [44, 45]. Although $P_{\mu e}^{NP}$ is suppressed by $|\alpha_{21}|^2$, which is smaller than 6.6×10^{-4} at 90% C.L., a near detector with a very short baseline can still collect enough number of events to provide information of this parameter.

We propose a near detector μ Near, with a 20 ton scintillator detector and a 20 m baseline to the μ DAR source, to supplement the μ Kam part of TNT2K. By selecting events with double coincidence, the scintillator can identify the oscillated electron anti-neutrinos. Most of the events come from two sources: the signal from μ^+ decay and the background from μ^- decay. For both signal and background, the parent muons decay at rest and hence have well-defined spectrum as shown in the left panel of Fig. 10. For a background-signal flux ratio $\mu^- \text{DAR} / \mu^+ \text{DAR} = 5 \times 10^{-4}$ [13] and non-unitary size $|\alpha_{21}| = 0.02$, the signal and background have roughly the same number of events, $N_{sig} = 1446$ and $N_{bkg} = 1234$. If the neutrino mixing is unitary, only background is present. Based on this we can roughly estimate the sensitivity at μ Near to be, $\sqrt{N_{bkg}}/N_{sig} \approx 2.4\%$, for $|\alpha_{21}|^2 = (0.02)^2$. When converted to $|\alpha_{21}|$, the limit can be improved by a factor of $1/\sqrt{2.4\%} \approx 6.5$ on the basis of 0.02 around 1σ . In addition, the spectrum shape is quite different between the signal and background. The signal peak appears around 50 MeV where the background event rate is much smaller. This feature of different energy spectrum can further enhance the sensitivity than the rough estimation from total event rate. The constraint on $|\alpha_{21}|$ can be significantly improved beyond the current limit in (6).

In the right panel of Fig. 10 we show the sensitivity on $|\alpha_{21}|$ as a function of the background rate and the detector size from a simplified template fit. The result for 5×10^{-4} of background and 20 ton detector is of the same size as the rough estimation. The concrete

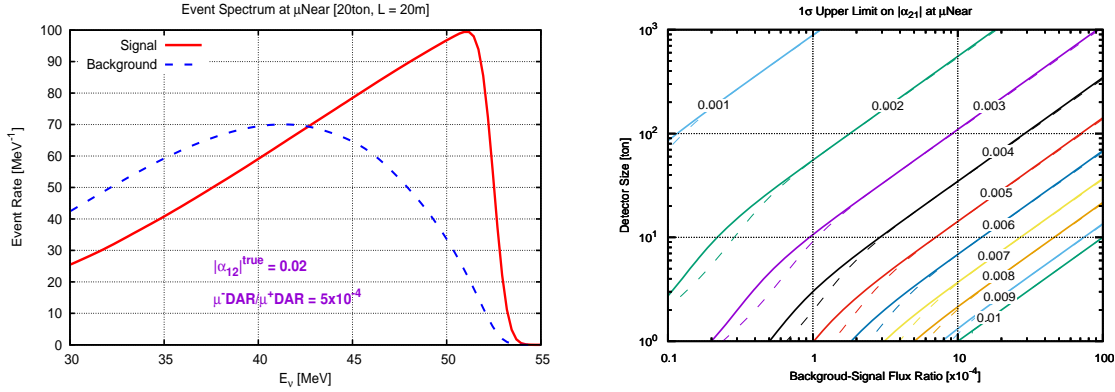


FIG. 10. Event rates (left panel) and the sensitivity on $|\alpha_{21}|$ (right panel) at μ Near as a function of background rate and detector size. For the sensitivity plot the solid contours are obtained with both 20% uncertainty in the μ DAR flux normalization and 50% uncertainty in the background-signal flux ratio. In contrast, the dashed contours are obtained with only 20% uncertainty in the μ DAR flux normalization while the background-signal flux ratio is fixed.

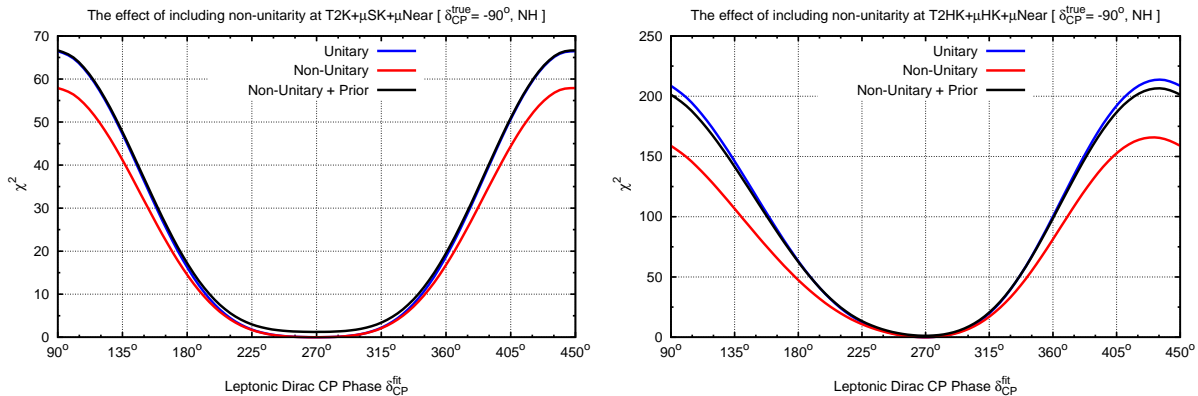


FIG. 11. The marginalized $\chi^2(\delta_{CP})$ function at TNT2K + μ Near under the assumptions of unitarity (blue), non-unitary mixing with (black) or without (red) prior constraints.

value, $|\alpha_{21}| < 0.004$ at 1σ , is lightly larger due to marginalization. In Fig. 10 we assumed systematic errors to be 20% for the μ DAR flux normalization and 50% for the background-signal flux ratio. The solid contours in the right panel are obtained with both systematic errors imposed while the dashed ones with only the 20% uncertainty in flux normalization. The difference in the sensitivity on $|\alpha_{21}|$ only appears in the region of small detector size or small background rate. For the 20 ton detector and background rate larger than 10^{-4} , the difference is negligibly small. In the full simulation, we only implement the 20% uncertainty in flux normalization for simplicity. In Fig. 11 we show the CP sensitivity at TNT2K plus μ Near once a full simulation is performed. Imposing all the information we can get from TNT2K, μ Near, and the prior constraints on the non-unitary mixing parameters (6), the

CP sensitivity can match the full potential of TNT2K under the assumption of unitary mixing. Even without prior constraints, the CP sensitivity at TNT2K plus μNear is very close to the full reach of TNT2K with unitary mixing. This combination of CP measurements, TNT2K plus μNear , can determine the leptonic Dirac CP phase δ_{CP} unambiguously and hence provide an ultimate solution to the degeneracy between unitary and non-unitary CP violation parameters.

VI. CONCLUSION

Our interpretation of experimental data always relies on theoretical assumptions. Unambiguous understanding of reality always requires distinguishing alternative assumptions through careful experimental design. The degeneracy between unitary and non-unitary CP phases in neutrino mixing provides a perfect example. In this paper we have confirmed, in agreement with Ref. [21], that, for values of $|\alpha_{21}|$ of the order of a few%, one can have unitarity violating CP oscillation amplitudes of the same order, or possibly larger, than the standard one associated to δ_{CP} . We have illustrated how the CP sensitivity at accelerator neutrino experiments like T2(H)K is severely degraded in the presence of non-unitarity. Indeed, in addition to the standard leptonic Dirac CP phase δ_{CP} if neutrino mixing is non-unitary there is an extra CP phase ϕ characterizing deviations from unitarity and affecting the neutrino appearance probability. The effect of such unitary phase δ_{CP} can be easily faked by the non-unitarity phase ϕ if only the $\sin \delta_{CP}$ dependence is probed, as in the T2(H)K configuration. Probing the interplay with the $\cos \delta_{CP}$ dependence can help to lift the degeneracy. A perfect solution comes from the TNT2K project with T2(H)K supplemented by a μDAR source. Thanks to the different energy scale of the accelerator and μDAR neutrino fluxes, two different measurements can proceed at the same time, using Super-K and Hyper-K detectors simultaneously. In its original proposal, the goal was to get better measurement of the Dirac CP phase δ_{CP} within the standard three-neutrino mixing benchmark. We find that it also has the potential of breaking the degeneracy between standard and non-unitary CP phases. However, TNT2K can fully explore its advantage only in combination with a near detector. We propose using μNear , with only 20 ton of scintillator and 20 m of baseline, to monitor the size of the non-unitary CP violating term for the $\mu \rightarrow e$ transition, $|\alpha_{21}|$. Our simplified template fit shows that μNear , with an expected background-signal flux ratio in the μDAR source of 5×10^{-4} , can constrain $|\alpha_{21}|$ to be smaller than 4×10^{-3} at 1σ , which corresponds to almost one order of magnitude improvement with respect to the current bound. This estimate is stable against the large uncertainty in the background-signal flux ratio. When implemented in a full simulation, μNear can almost retrieve the CP sensitivity of TNT2K, providing an ultimate solution to the degeneracy between unitary and

non-unitary mixing parameters.

In short, non-unitary neutrino mixing is expected in a large class of seesaw schemes at LHC-accessible mass scales. This implies extra mixing parameters, and a new CP phase, that can fake the standard leptonic CP phase δ_{CP} present in the simplest three-neutrino paradigm. As a result, probing for CP violation in accelerator-type experiments can be misleading. We have considered T2(H)K as an example to illustrate the degeneracy between the “standard” and “non-unitary” CP phases. Despite the complete loss in its CP sensitivity we note that supplementing T2(H)K with a μ DAR source can help breaking the CP degeneracy, by probing separately both $\cos \delta_{CP}$ and $\sin \delta_{CP}$ dependences in the wide energy spectrum of the μ DAR flux. We have seen that the further addition of a near detector to the μ DAR setup has the potential of removing the degeneracy rather well.

VII. ACKNOWLEDGEMENTS

Work supported by Spanish grants FPA2014-58183-P, Multidark CSD2009-00064, SEV-2014-0398 (MINECO), PROMETEOII/2014/084 (Generalitat Valenciana). M. T. is supported by a Ramón y Cajal contract (MINECO). P. S. P. would like to thank the support of FAPESP funding grant 2014/05133-1 and 2015/16809-9. SFG thanks Jarah Evslin for useful discussions.

Appendix A: Decomposition Formalism for Non-Unitary Mixing

The parametrization in Eq. (4) isolates the effect of non-unitarity as a multiplicative matrix on the left-hand side of the unitary mixing matrix U . This choice is extremely convenient to separate the neutrino oscillation probabilities into several terms, using the decomposition formalism [47]. The latter has a huge benefit for the case of non-unitary mixing, characterized by the parameters α_{ij} in N^{NP} . Indeed it simplifies considerably the calculation of the oscillation amplitudes as we demonstrate below.

Neglecting the matter potential, we have the effective Hamiltonian

$$\mathcal{H}^{NP} = \frac{1}{2E_\nu} N \begin{pmatrix} 0 & & \\ & \Delta m_s^2 & \\ & & \Delta m_a^2 \end{pmatrix} N^\dagger = N^{NP} \mathcal{H} N^{NP\dagger}, \quad (\text{A1})$$

Notice how it relates to its standard counterpart \mathcal{H} with unitary mixing matrix U , through a basis transformation N^{NP} on both sides. This implies for the evolution operator the same relation, namely

$$S^{NP} = N^{NP} S N^{NP\dagger}, \quad (\text{A2})$$

where S is the standard amplitude matrix corresponding to unitary mixing U . Note that the extra neutrinos are much heavier than the energy scale under discussion and hence decouple from the (low-energy) neutrino oscillations. Their low-energy effect is just a basis transformation which also applies to the oscillation amplitudes. The neutrino oscillation probability is given by the squared magnitude of the corresponding amplitude matrix element, $P_{\alpha\beta}^{NP} = |S_{\beta\alpha}^{NP}|^2$,

$$P_{ee}^{NP} = \alpha_{11}^4 P_{ee}, \quad (\text{A3a})$$

$$P_{e\mu}^{NP} = \alpha_{11}^2 [\alpha_{22}^2 P_{e\mu} + 2\alpha_{22} \text{Re}(\alpha_{21} S_{ee}^* S_{\mu e}) + |\alpha_{21}|^2 P_{ee}], \quad (\text{A3b})$$

$$P_{\mu e}^{NP} = \alpha_{11}^2 [\alpha_{22}^2 P_{\mu e} + 2\alpha_{22} \text{Re}(\alpha_{21}^* S_{ee} S_{e\mu}^*) + |\alpha_{21}|^2 P_{ee}], \quad (\text{A3c})$$

$$P_{\mu\mu}^{NP} = \alpha_{22}^4 P_{\mu\mu} + |\alpha_{21}|^2 \alpha_{22}^2 (P_{\mu e} + P_{e\mu}) + |\alpha_{21}|^4 P_{ee} \\ + \sum_{\{a_1, b_1\} \neq \{a_2, b_2\}} \text{Re}[\alpha_{2a_1} \alpha_{2b_1}^* \alpha_{2a_2}^* \alpha_{2b_2} S_{a_1 b_1} S_{a_2 b_2}^*]. \quad (\text{A3d})$$

Here $P_{\alpha\beta}$ is the oscillation probability with unitary mixing and $(a, b)=(1, 2)$ for α_{ab} while $(a, b)=(e, \mu)$ for S_{ab} . Note that the remaining five oscillation probabilities ($P_{e\tau}^{NP}$, $P_{\tau e}^{NP}$, $P_{\mu\tau}^{NP}$, $P_{\tau\mu}^{NP}$, $P_{\tau\tau}^{NP}$) can not be derived from the four in (A3) by unitarity conditions since these do not hold in our case. Instead, they need to be calculated directly from S^{NP} elements in a similar way as the above four.

In addition, the atmospheric mixing angle and the Dirac CP phase δ_{CP} can also be factorized out as transformations,

$$\mathcal{H} = [U_{23}(\theta_a) P_\delta] \mathcal{H}' [U_{23}(\theta_a) P_\delta]^\dagger, \quad S = [U_{23}(\theta_a) P_\delta] S' [U_{23}(\theta_a) P_\delta]^\dagger, \quad (\text{A4})$$

where $U_{23}(\theta_a)$ is the 2–3 mixing parameter and $P_\delta \equiv \text{diag}(1, 1, e^{i\delta_{CP}})$ is a rephasing matrix. Those quantities with prime, \mathcal{H}' and S' , are defined in the so-called ‘‘propagation basis’’ [48, 49]. The connection between the non-unitary flavor basis and the ‘‘propagation basis’’ is $N^{NP} U_{23}(\theta_a) P_\delta$. Replacing the unitary oscillation amplitude S in the flavor basis by S' [47] in the ‘‘propagation basis’’ with θ_a and δ_{CP} rotated away, the non-unitary oscillation probabilities (A3) become,

$$P_{ee}^{NP} = \alpha_{11}^4 P_{ee}, \quad (\text{A5a})$$

$$P_{e\mu}^{NP} = \alpha_{11}^2 \{ \alpha_{22}^2 P_{e\mu} + 2\alpha_{22} |\alpha_{21}| [c_\phi (\mathbb{R} + s_\phi \mathbb{I}) (S'_{11} S'_{21}^*) \\ + s_a (c_{\phi+\delta_{CP}} \mathbb{R} + s_{\phi+\delta_{CP}} \mathbb{I}) (S'_{11} S'_{31}^*)] + |\alpha_{21}|^2 P_{ee} \}, \quad (\text{A5b})$$

$$P_{\mu e}^{NP} = \alpha_{11}^2 \{ \alpha_{22}^2 P_{\mu e} + 2\alpha_{22} |\alpha_{21}| [c_\phi (\mathbb{R} - s_\phi \mathbb{I}) (S'_{11} S'_{12}^*) \\ + s_a (c_{\phi+\delta_{CP}} \mathbb{R} - s_{\phi+\delta_{CP}} \mathbb{I}) (S'_{11} S'_{13}^*)] + |\alpha_{21}|^2 P_{ee} \}, \quad (\text{A5c})$$

$$P_{\mu\mu}^{NP} = |\alpha_{22}^2 S_{\mu\mu} + \alpha_{22} (\alpha_{21} S_{e\mu} + \alpha_{21}^* S_{\mu e}) + \alpha_{11}^2 S_{ee}|^2 \quad (\text{A5d})$$

For convenience, we have denoted $(c_\phi, s_\phi) \equiv (\cos \phi, \sin \phi)$ and $(c_{\phi+\delta_{CP}}, s_{\phi+\delta_{CP}}) \equiv (\cos(\phi + \delta_{CP}), \sin(\phi + \delta_{CP}))$, where δ_{CP} and ϕ are the leptonic Dirac CP phase and the non-unitary

	$P_{ee}^{(k)}$	$P_{e\mu}^{(k)}$	$P_{\mu e}^{(k)}$
(0)	$\alpha_{11}^4 S'_{11} ^2$	$\alpha_{11}^2 \left[\frac{\alpha_{22}^2}{2} (1 - S'_{11} ^2) + \alpha_{21} ^2 S'_{11} ^2 \right]$	$\alpha_{11}^2 \left[\frac{\alpha_{22}^2}{2} (1 - S'_{11} ^2) + \alpha_{21} ^2 S'_{11} ^2 \right]$
(1)	0	$\frac{\alpha_{11}^2 \alpha_{22}^2}{2} (S'_{21} ^2 - S'_{31} ^2)$	$\frac{\alpha_{11}^2 \alpha_{22}^2}{2} (S'_{12} ^2 - S'_{13} ^2)$
(2)	0	$\alpha_{11}^2 \alpha_{22}^2 \mathbb{R}(S'_{21} S'_{31}^*)$	$\alpha_{11}^2 \alpha_{22}^2 \mathbb{R}(S'_{12} S'_{13}^*)$
(3)	0	$\alpha_{11}^2 \alpha_{22}^2 \mathbb{I}(S'_{21} S'_{31}^*)$	$-\alpha_{11}^2 \alpha_{22}^2 \mathbb{I}(S'_{12} S'_{13}^*)$
(4)	0	0	0
(5)	0	0	0
(6)	0	0	0
(7)	0	$+2\alpha_{11}^2 \alpha_{22} \alpha_{21} \mathbb{R}(S'_{11} S'_{21}^*)$	$+2\alpha_{11}^2 \alpha_{22} \alpha_{21} \mathbb{R}(S'_{11} S'_{12}^*)$
(8)	0	$+2\alpha_{11}^2 \alpha_{22} \alpha_{21} \mathbb{I}(S'_{11} S'_{21}^*)$	$-2\alpha_{11}^2 \alpha_{22} \alpha_{21} \mathbb{I}(S'_{11} S'_{12}^*)$
(9)	0	$+2\alpha_{11}^2 \alpha_{22} \alpha_{21} \mathbb{R}(S'_{11} S'_{31}^*)$	$+2\alpha_{11}^2 \alpha_{22} \alpha_{21} \mathbb{R}(S'_{11} S'_{13}^*)$
(10)	0	$+2\alpha_{11}^2 \alpha_{22} \alpha_{21} \mathbb{I}(S'_{11} S'_{31}^*)$	$-2\alpha_{11}^2 \alpha_{22} \alpha_{21} \mathbb{I}(S'_{11} S'_{13}^*)$

TABLE I. The decomposed coefficients $P_{ee}^{(k)}$, $P_{e\mu}^{(k)}$, and $P_{\mu e}^{(k)}$ as an extension to the results first derived in [47]. For symmetric matter potential profile, the amplitude matrix S' is also symmetric.

phase associated with $\alpha_{21} \equiv |\alpha_{21}|e^{-i\phi}$, respectively. The real and imaginary operators, \mathbb{R} and \mathbb{I} , extract the corresponding part of the following terms. The general expression (A5) reproduces the fully expanded form in [20] up to the leading order of $\sin \theta_r \sim 0.15$ and $\Delta m_s^2/\Delta m_a^2 \sim 3\%$.

The oscillation probabilities $P_{e\mu}^{NP}$ and $P_{\mu e}^{NP}$ in (A5) are not just functions of their unitary counterparts $P_{e\mu}$ and $P_{\mu e}$, but they also contain non-unitary CP terms involving ϕ . Therefore, the non-unitarity of the neutrino mixing matrix introduces extra decomposition coefficients in addition to those proposed in [47],

$$\begin{aligned}
P_{\alpha\beta}^{NP} \equiv & P_{\alpha\beta}^{(0)} + P_{\alpha\beta}^{(1)} x_a + P_{\alpha\beta}^{(2)} \cos \delta'_{CP} + P_{\alpha\beta}^{(3)} \sin \delta'_{CP} + P_{\alpha\beta}^{(4)} x_a \cos \delta'_{CP} + P_{\alpha\beta}^{(5)} x_a^2 + P_{\alpha\beta}^{(6)} \cos^2 \delta'_{CP} \\
& + P_{\alpha\beta}^{(7)} c_a c_\phi + P_{\alpha\beta}^{(8)} c_a s_\phi + P_{\alpha\beta}^{(9)} s_a c_{\phi+\delta_{CP}} + P_{\alpha\beta}^{(10)} s_a s_{\phi+\delta_{CP}}.
\end{aligned} \tag{A6}$$

Here, we have expanded the atmospheric angle θ_a around its maximal value $c_a^2 = (1 + x_a)/2$ and rescaled Dirac CP functions ($\cos \delta'_{CP}, \sin \delta'_{CP}$) $\equiv 2c_a s_a (\cos \delta_{CP}, \sin \delta_{CP})$. The explicit form of these decomposition coefficients are shown in Tab. I. For simplicity, we show just the three channels (P_{ee}^{NP} , $P_{e\mu}^{NP}$, and $P_{\mu e}^{NP}$) in Tab. I to illustrate the idea. Ignoring matter effects (or if these can be approximated by a symmetric/constant potential), the amplitude matrix S' is then symmetric, $S'_{ij} = S'_{ji}$. To obtain the anti-neutrino coefficients $\overline{P}_{\alpha\beta}^{NP}$, the CP phases (δ_{CP} and ϕ) as well as the matter potential inside the S' matrix elements should receive a minus sign.

Appendix B: Matter effect with non-unitary mixing

The decomposition formalism presented in App. A is a powerful tool to obtain a complete formalism for neutrino oscillations. It factorizes the mixings efficiently in different bases and treats their effects independently. For example, the matter potential does not spoil the relations (A3) that follow from the general parametrization (4). Although the previous results are obtained for vacuum oscillations, one can still use (A3) for neutrino oscillation through matter, as long as S_{ij} is replaced by the corresponding amplitude matrix in matter, S_{ij}^{matter} . In this appendix we will show how the presence of non-unitary neutrino mixing results in a rescaling of the standard matter potential.

In order to further develop the formalism established in App. A to introduce matter effects with non-unitary mixing, it is extremely useful to use the symmetrical parametrization method for unitary matrices. We start by recalling that its main ingredient consists in decomposing $U^{n \times n}$ in terms of products of effectively two-dimensional complex rotation matrices ω_{1j} , in which each factor is characterized by both one rotation angle and one CP phase, see Eqs.(3.9)–(3.15) and (3.19)–(3.22) in [7]. The method is equivalent to the procedure of obtaining the current PDG form of the lepton mixing matrix and any generalization thereof. In the presence of $SU(3)_c \otimes SU(2)_L \otimes U(1)_Y$ singlet neutrinos, it can be used to describe the mixing matrix $U^{n \times n}$ as follows

$$U^{n \times n} = \left(\prod_{i>j>3}^n \omega_{ij} \right) \left(\prod_{j=4}^n \omega_{3j} \right) \left(\prod_{j=4}^n \omega_{2j} \right) \begin{pmatrix} \omega_{23} P_\delta & 0 \\ 0 & 1 \end{pmatrix} \left(\prod_{j=4}^n \omega_{1j} \right) \begin{pmatrix} \omega_{13} \omega_{12} & 0 \\ 0 & 1 \end{pmatrix}. \quad (\text{B1})$$

in the same way as for its 3×3 counterpart U . The non-unitarity contribution has been decomposed into four parts of which the last term $\prod_{j=4}^n \omega_{1j}$ can be seen to commute with $\omega_{23} P_\delta$. Notice that the matter effects can only affect the electron flavor [36] which commute with P_δ and ω_{ij} as long as $i, j \neq 1$. In other words, within such decomposition formalism for the extended mixing matrix, one can still set up a temporary basis that is connected to the non-unitary flavor basis with the transformation matrix

$$\mathcal{R}'' = \left(\prod_{i>j>3}^n \omega_{ij} \right) \left(\prod_{j=4}^n \omega_{3j} \right) \left(\prod_{j=4}^n \omega_{2j} \right) \begin{pmatrix} \omega_{23} P_\delta & 0 \\ 0 & 1 \end{pmatrix}. \quad (\text{B2})$$

The remaining part of the mixing matrix contains rotations ω_{1j} with all possible values of $2 \leq j \leq n$, and the standard Dirac CP phase δ_{CP} . For convenience, let us denote the mixing matrix in this temporary basis as,

$$U'' \equiv \left(\prod_{j=4}^n \omega_{1j} \right) \begin{pmatrix} \omega_{13} \omega_{12} & 0 \\ 0 & 1 \end{pmatrix} \equiv U''_{NP} \begin{pmatrix} \omega_{13} \omega_{12} & 0 \\ 0 & 1 \end{pmatrix}. \quad (\text{B3})$$

Correspondingly, the oscillation amplitude matrix is,

$$i\partial_L \mathcal{S}'' = U'' \begin{pmatrix} \sqrt{E^2 - m_1^2} & & \\ & \ddots & \\ & & \sqrt{E^2 - M_n^2} \end{pmatrix} U''^\dagger + \begin{pmatrix} V & & \\ & 0 & \\ & & \ddots \end{pmatrix}, \quad (\text{B4})$$

For heavy mass eigenstates with $M_i > M_Z \gg E$, the oscillation will decay out very quickly since the oscillation phase $\sqrt{E^2 - M_n^2}$ is imaginary.

For convenience, we separate the matrices into light and heavy blocks,

$$i\partial_L \mathcal{S}'' = U''_{NP} \left[\begin{pmatrix} \sqrt{E^2 - \mathbb{M}_l^2} & \\ & \sqrt{E^2 - \mathbb{D}_h^2} \end{pmatrix} + U''_{NP}^\dagger \begin{pmatrix} V & \\ & 0 \end{pmatrix} U''_{NP} \right] U''_{NP}^\dagger \quad (\text{B5})$$

where $\sqrt{E^2 - \mathbb{M}_l^2}$ is the standard momentum matrix in the ‘‘propagation basis’’, with the solar and reactor angles θ_s and θ_r incorporated, while $\sqrt{E^2 - \mathbb{D}_h^2}$ is already diagonal. As long as $V \ll \sqrt{E^2 - \mathbb{D}_h^2}$, the mixing between the light and heavy blocks inside the bracket is highly suppressed by a factor of $V/\sqrt{E^2 - \mathbb{D}_h^2}$. For CP measurement experiments, $V \lesssim \Delta m_a^2/2E \ll \sqrt{E^2 - \mathbb{D}_h^2}$ with $\Delta m_a^2 \sim \mathcal{O}(0.01 \text{ eV}^2)$, $10 \text{ MeV} \lesssim E \lesssim 1 \text{ GeV}$, and $\mathbb{D}_h^2 > M_Z^2$, the induced mixing $V/\sqrt{E^2 - \mathbb{D}_h^2} \lesssim 10^{-19}$ is negligibly small. In addition, the mixing term is further suppressed by the small non-unitary mixing contained in U''_{NP} . As a good approximation for low-energy neutrino oscillation experiment, the light and heavy blocks decouple from each other.

Consequently, the non-unitary mixing U''_{NP} in the temporary basis can be simply factorized out since U''_{NP} in (B5) appears as an overall rotation. The transformation matrix (B2) is then replaced by

$$\mathcal{R}' = (\Pi_{i>j>3}^n \omega_{ij}) (\Pi_{j=4}^n \omega_{3j}) (\Pi_{j=4}^n \omega_{2j}) (\Pi_{j=4}^n \omega_{1j}) \begin{pmatrix} \omega_{23} P_\delta & 0 \\ 0 & 1 \end{pmatrix}, \quad (\text{B6})$$

to establish the ‘‘propagation basis’’ [48, 49] in the presence of non-unitary mixing. Note that \mathcal{R}' is exactly $N^{NP} U_{23}(\theta_a) P_\delta$ that already used in App. A to relate the non-unitary flavor basis and the ‘‘propagation basis’’ through (A2) and (A4). In other words, as long as the mass of heavy neutrino is much larger than the oscillation energy and matter effect, the same ‘‘propagation basis’’ can be generalized for non-unitary mixing.

Since the light and heavy blocks effectively decouple from each other, the oscillation probability can be evaluated independently. For the light block, we can first evaluate the amplitude matrix S' in the ‘‘propagation basis’’ and transform back to the flavor basis with \mathcal{R}' in the same way as (A5). The only change is a modified matter potential,

$$\tilde{\mathbb{M}}_l^2 = \mathbb{M}_l^2 - 2E U''_{NP}^\dagger V U''_{NP}, \quad (\text{B7})$$

where U''_{NP} is the light block of U''_{NP} . Here we have expanded the neutrino momentum of light neutrinos in relativistic limit. The potential matrix in the “propagation basis” is replaced by $V \rightarrow U''_{NP\dagger} V U''_{NP}$. Note that this applies for both standard and non-standard interactions. For standard matter potential, the last term is equivalent to a rescaling, $V \rightarrow \alpha_{11} V$.

-
- [1] G. Branco, R. G. Felipe, and F. Joaquim, *Rev.Mod.Phys.* **84**, 515 (2012), arXiv:1111.5332 [hep-ph].
 - [2] P. Chen, G.-J. Ding, F. Gonzalez-Canales, and J. W. F. Valle, (2016), arXiv:1604.03510 [hep-ph].
 - [3] P. Chen, G.-J. Ding, F. Gonzalez-Canales, and J. W. F. Valle, *Phys. Lett.* **B753**, 644 (2016), arXiv:1512.01551 [hep-ph].
 - [4] S. Morisi and J. W. F. Valle, *Fortsch.Phys.* **61**, 466 (2013), arXiv:1206.6678 [hep-ph].
 - [5] S. F. King, A. Merle, S. Morisi, Y. Shimizu, and M. Tanimoto, *New J. Phys.* **16**, 045018 (2014), arXiv:1402.4271 [hep-ph].
 - [6] M. Kobayashi and T. Maskawa, *Prog. Theor. Phys.* **49**, 652 (1973).
 - [7] J. Schechter and J. W. F. Valle, *Phys. Rev.* **D22**, 2227 (1980).
 - [8] L. Wolfenstein, *Phys. Rev. Lett.* **51**, 1945 (1983).
 - [9] M. Maltoni, T. Schwetz, M. Tortola, and J. Valle, *New J.Phys.* **6**, 122 (2004), arXiv:hep-ph/0405172 [hep-ph].
 - [10] D. V. Forero, M. Tortola, and J. W. F. Valle, *Phys. Rev.* **D90**, 093006 (2014), arXiv:1405.7540 [hep-ph].
 - [11] K. Abe *et al.* (T2K), *Phys. Rev.* **D91**, 072010 (2015), arXiv:1502.01550 [hep-ex].
 - [12] K. Abe *et al.*, (2011), arXiv:1109.3262 [hep-ex].
 - [13] J. Evslin, S.-F. Ge, and K. Hagiwara, *JHEP* **02**, 137 (2016), arXiv:1506.05023 [hep-ph].
 - [14] R. N. Mohapatra and J. W. F. Valle, *Phys. Rev.* **D34**, 1642 (1986).
 - [15] M. Gonzalez-Garcia and J. Valle, *Phys.Lett.* **B216**, 360 (1989).
 - [16] E. K. Akhmedov, M. Lindner, E. Schnapka, and J. W. F. Valle, *Phys. Rev.* **D53**, 2752 (1996), arXiv:hep-ph/9509255 [hep-ph].
 - [17] E. K. Akhmedov, M. Lindner, E. Schnapka, and J. Valle, *Phys.Lett.* **B368**, 270 (1996), arXiv:hep-ph/9507275 [hep-ph].
 - [18] M. Malinsky, J. Romao, and J. Valle, *Phys.Rev.Lett.* **95**, 161801 (2005), arXiv:hep-ph/0506296 [hep-ph].
 - [19] F. Bazzocchi, *Phys.Rev.* **D83**, 093009 (2011), arXiv:1011.6299 [hep-ph].

- [20] F. J. Escrivuela, D. V. Forero, O. G. Miranda, M. Tortola, and J. W. F. Valle, Phys. Rev. **D92**, 053009 (2015), arXiv:1503.08879 [hep-ph].
- [21] O. G. Miranda, M. Tortola, and J. W. F. Valle, (2016), arXiv:1604.05690 [hep-ph].
- [22] O. G. Miranda and J. W. F. Valle, (2016), arXiv:1602.00864 [hep-ph].
- [23] S.-F. Ge, H.-J. He, and F.-R. Yin, JCAP **1005**, 017 (2010), arXiv:1001.0940 [hep-ph].
- [24] D. A. Dicus, S.-F. Ge, and W. W. Repko, Phys. Rev. **D83**, 093007 (2011), arXiv:1012.2571 [hep-ph].
- [25] S.-F. Ge, D. A. Dicus, and W. W. Repko, Phys. Lett. **B702**, 220 (2011), arXiv:1104.0602 [hep-ph].
- [26] S.-F. Ge, D. A. Dicus, and W. W. Repko, Phys. Rev. Lett. **108**, 041801 (2012), arXiv:1108.0964 [hep-ph].
- [27] A. D. Hanlon, S.-F. Ge, and W. W. Repko, Phys. Lett. **B729**, 185 (2014), arXiv:1308.6522 [hep-ph].
- [28] J. Bernabeu *et al.*, Phys. Lett. **B187**, 303 (1987).
- [29] G. C. Branco, M. N. Rebelo, and J. W. F. Valle, Phys. Lett. **B225**, 385 (1989).
- [30] N. Rius and J. W. F. Valle, Phys. Lett. **B246**, 249 (1990).
- [31] F. Deppisch and J. W. F. Valle, Phys. Rev. **D72**, 036001 (2005), hep-ph/0406040.
- [32] F. Deppisch, T. S. Kosmas, and J. W. F. Valle, Nucl. Phys. **B752**, 80 (2006), hep-ph/0512360.
- [33] F. F. Deppisch, N. Desai, and J. W. F. Valle, Phys.Rev. **D89**, 051302(R) (2014), arXiv:1308.6789 [hep-ph].
- [34] S. Das, F. Deppisch, O. Kittel, and J. W. F. Valle, Phys.Rev. **D86**, 055006 (2012), arXiv:1206.0256 [hep-ph].
- [35] S. Mikheev and A. Smirnov, Sov.J.Nucl.Phys. **42**, 913 (1985).
- [36] L. Wolfenstein, Phys.Rev. **D17**, 2369 (1978).
- [37] S.-F. Ge, NuPro: a simulation package for neutrino properties, <http://nupro.hepforge.org> (to appear).
- [38] J. W. Valle and J. C. Romao, *Neutrinos in high energy and astroparticle physics* (John Wiley & Sons, 2015, ISBN: 978-3-527-41197-9).
- [39] K. A. Olive *et al.* (Particle Data Group), Chin. Phys. **C38**, 090001 (2014).
- [40] J. Schechter and J. W. F. Valle, Phys. Rev. **D23**, 1666 (1981).
- [41] M. Doi, T. Kotani, H. Nishiura, K. Okuda, and E. Takasugi, Phys. Lett. **B102**, 323 (1981).
- [42] J. Schechter and J. Valle, Phys.Rev. **D25**, 2951 (1982).
- [43] J. Schechter and J. W. F. Valle, Phys. Rev. **D25**, 774 (1982).
- [44] J. W. F. Valle, Phys. Lett. **B199**, 432 (1987).
- [45] H. Nunokawa *et al.*, Phys. Rev. **D54**, 4356 (1996), hep-ph/9605301.

- [46] S. Antusch, C. Biggio, E. Fernandez-Martinez, M. B. Gavela, and J. Lopez-Pavon, *JHEP* **10**, 084 (2006), arXiv:hep-ph/0607020 [hep-ph].
- [47] S.-F. Ge, K. Hagiwara, and C. Rott, *JHEP* **06**, 150 (2014), arXiv:1309.3176 [hep-ph].
- [48] E. K. Akhmedov, A. Dighe, P. Lipari, and A. Y. Smirnov, *Nucl. Phys.* **B542**, 3 (1999), arXiv:hep-ph/9808270 [hep-ph].
- [49] H. Yokomakura, K. Kimura, and A. Takamura, *Phys. Lett.* **B544**, 286 (2002), arXiv:hep-ph/0207174 [hep-ph].